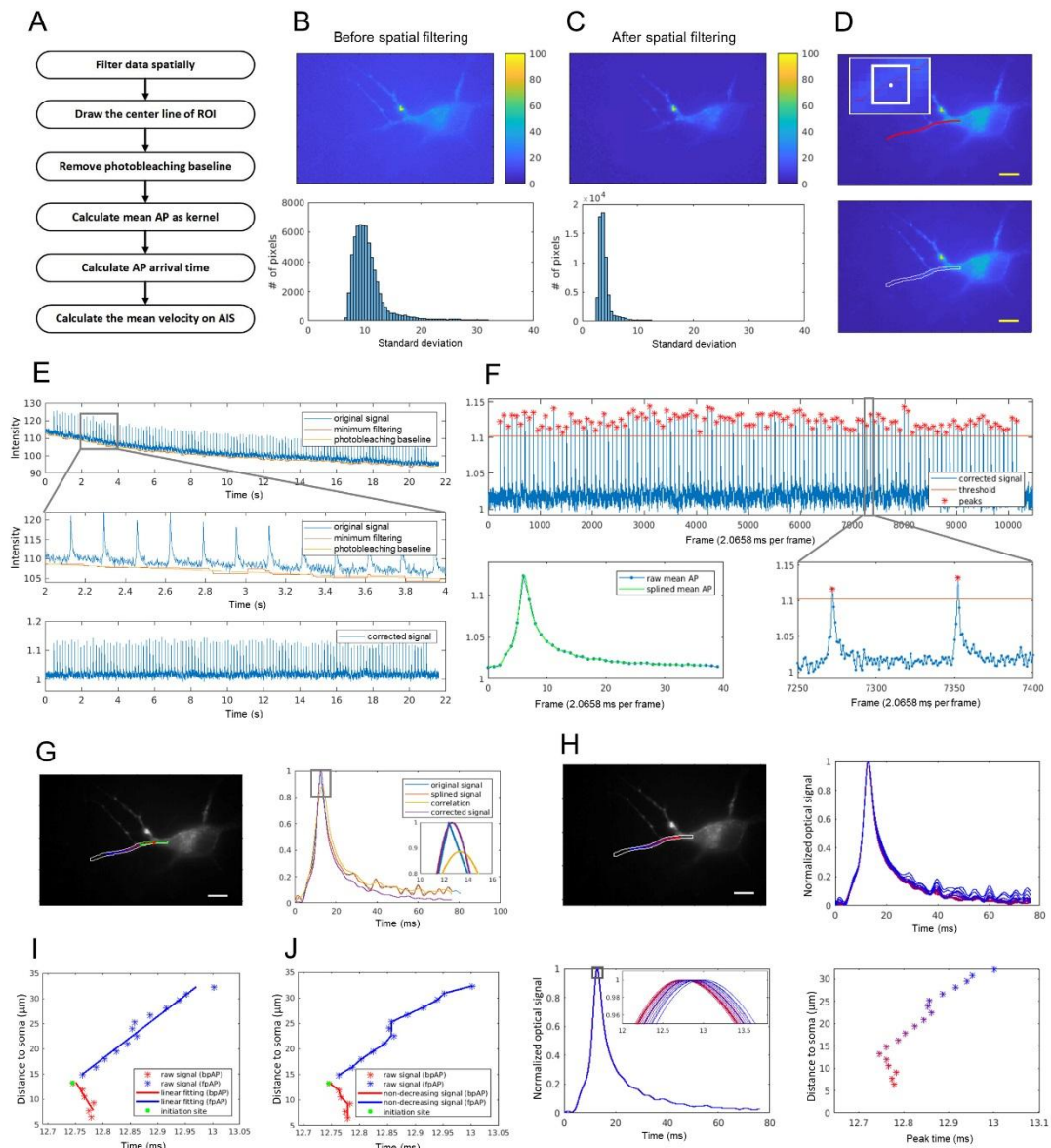


Supplementary Materials



Supplementary Figure S1 Process of calculating propagation speed from raw data

Data processing method was used to extract AP speed from raw voltage imaging data, including: spatially filtering data, drawing centerline of ROI, removing photobleaching baseline, calculating mean AP as kernel, calculating AP arrival time, and calculating mean speed on AIS.

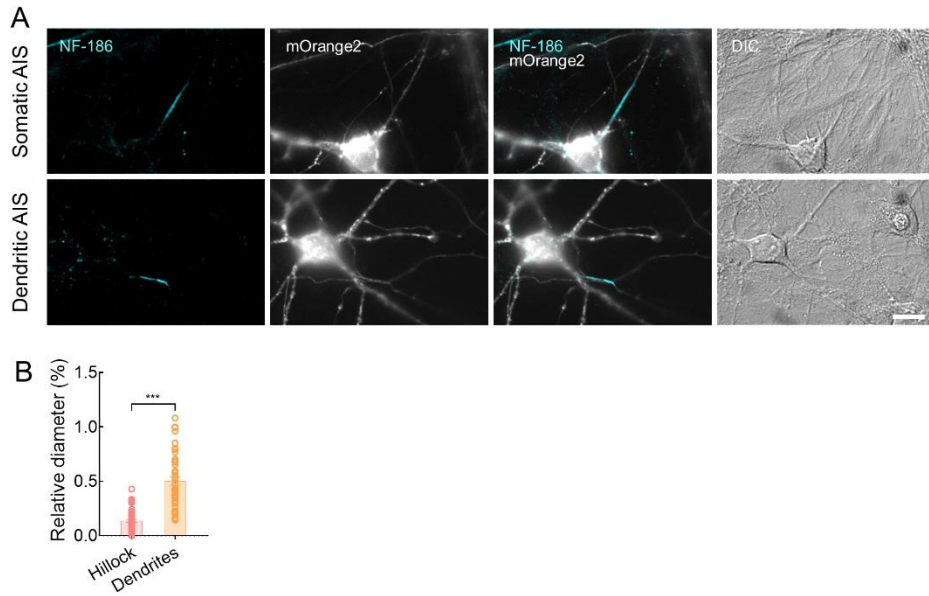
A. Flow chart of data processing method.

B. Upper image is raw image of a neuron, where value of each pixel is the standard deviation of intensity throughout voltage imaging. Lower image is the standard deviation histogram of the pixels in the upper image.

C. Upper image is an image of a neuron after spatial filtering, where value of each pixel is

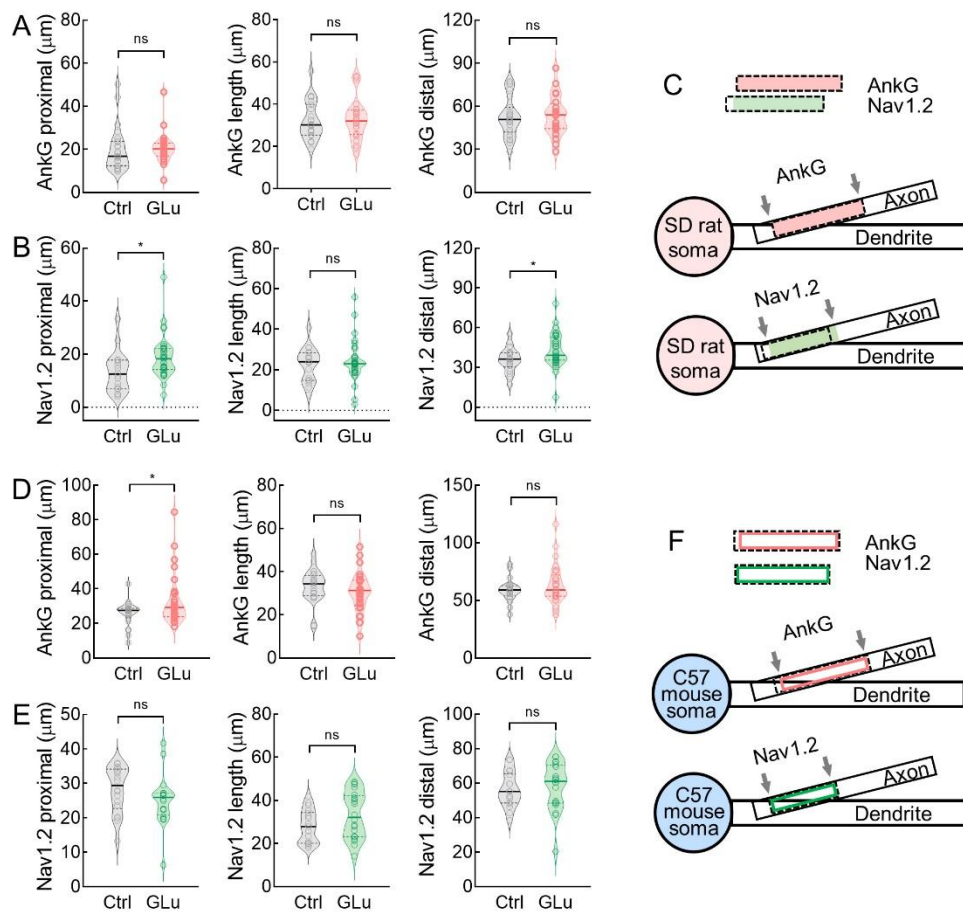
the standard deviation of intensity throughout voltage imaging. Lower image is the standard deviation histogram of the pixels in the upper image.

- D.** Upper image is intensity image of a neuron. Red line is the centerline of an axon drawn by the user. Inner image shows how ROI is delineated: size of white square is 5×5 ; window slides along red line, with center white point located on the red line; region slid by the window is the ROI. White line in lower image is ROI (Scale bar: $10 \mu\text{m}$).
- E.** Removal of photobleaching. Upper, blue line is the original (raw) signal of the ROI. Red line is the minimum filtering result of the blue line. Yellow line is the baseline of photobleaching calculated via a mean filter applied to the red line. Middle, larger image of gray square in the upper image. Lower, corrected signal of ROI ($\Delta F/F$) calculated by original signal (blue) divided by photobleaching baseline (yellow).
- F.** Mean AP calculation. Upper, peaks of each APs. Blue signal is corrected signal after removing the photobleaching baseline. Red line is a manual threshold; APs whose maximum voltage was higher than the threshold were considered normal and used to calculate mean AP. Red stars are peaks of each AP. Lower right image is larger image of the gray rectangle. Lower left image is mean AP, i.e., mean of all selected APs aligned with AP peaks.
- G.** Correct signals on each segment. Left, region circled by white line is ROI. Red and blue points are sampled locations in the axon. Green region is one segment with red-point center. Right, blue AP trace is the original signal, i.e., mean intensity of green region in left image. Red AP trace is interpolated from blue trace by cubic spline interpolation. Yellow AP trace is correlation function between blue and red traces. Purple AP trace is corrected signal, i.e., final result of this step.
- H.** Time-aligned corrected AP traces from different locations for a cell. Upper left, axon is circled with a white line. Points gradually changing from red (close to soma) and blue (far from soma), are in different locations in the axon. Upper right, normalized raw optical signals at each location. Lower left, corrected mean APs at each location. Inner figure is magnified gray rectangle, showing AP peaks. Lower right, peak time of APs at each location. Color of four images is consistent.
- I.** Mean speed calculation. Red and blue stars are peak times of bpAPs and fpAPs, respectively. Red and blue lines are linear fitting lines. Slopes of red and blue lines are mean speeds of bpAP and fpAP, respectively. Green point is initiation site.
- J.** Instantaneous speed calculation. Red and blue stars are peak times of bpAPs and fpAPs, respectively. Least-squares curve fitting was used to calculate red and blue curves with linear constraints. Slope of curves at each location is instantaneous speed at each position. Green point is initiation site.



Supplementary Figure S2 Representative images of distal-shifted AISs after KCl treatment in somatic AIS and dendritic AIS neurons.

- A.** Representative images of cultured wild-type rat hippocampal neurons (DIV12) after 48 h of treatment with 15 mmol/L KCl. All neurons were transfected at DIV7 with QuasAr2-mOrange2 plasmid. Selected neurons (white) and their AISs (blue) are indicated by fluorescence of mOrange2 and axonal marker NF-186, respectively. Corresponding DIC images correspond to neurons in left column (scale bars: 20 μ m).
- B.** Relative diameter of dendrites ($n=39$ was much thicker than that of hillock ($n=62$), ***: $P<0.001$).

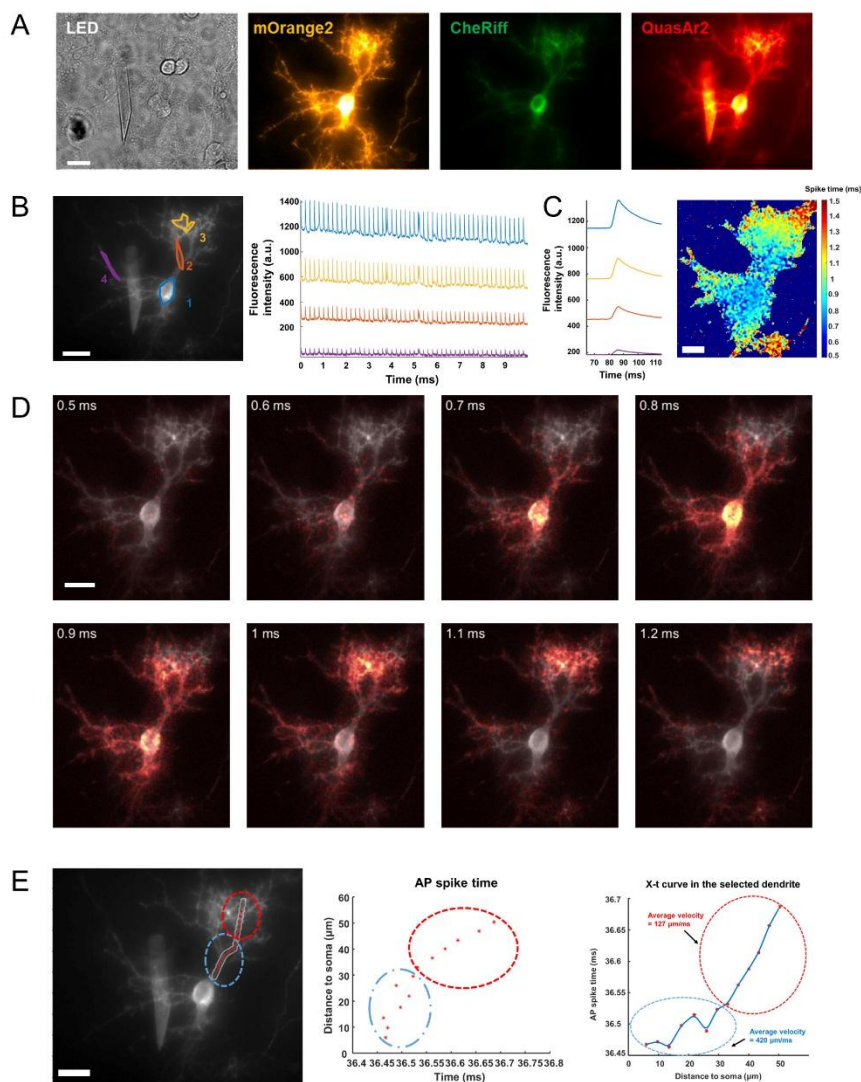


Supplementary Figure S3 AnkG and Nav1.2 length/location in dendritic AISs exhibited little change after treatment with 20 mmol/L glucose

- A.** In dendritic AIS neurons in rats, compared with control group (gray), both AIS location and length were similar to 3 h 20 mmol/L glucose-treated group (pink). Left, proximal end of AIS in 20 mmol/L glucose-treated group ($20.65 \pm 1.51 \mu\text{m}$, $n=24$) was similar to that in control group ($20.13 \pm 2.18 \mu\text{m}$, $n=23$), ns: $P > 0.05$. Middle, AIS length in 20 mmol/L glucose-treated group ($32.78 \pm 2.0 \mu\text{m}$, $n=24$) was similar to that in control group ($32.17 \pm 1.89 \mu\text{m}$, $n=23$), ns: $P > 0.05$. Right, distal end of AIS in 20 mmol/L glucose-treated group ($53.43 \pm 2.81 \mu\text{m}$, $n=24$) was similar to that in control group ($52.30 \pm 2.88 \mu\text{m}$, $n=23$), ns: $P > 0.05$.
- B.** In dendritic AIS neurons in rats, compared with control group (gray), Nav1.2 location showed significant distal shift but similar length in 3 h 20 mmol/L glucose-treated group (green). Left, proximal end of Nav1.2 in 20 mmol/L glucose-treated group ($18.88 \pm 1.30 \mu\text{m}$, $n=36$) was significantly further from soma than that in control group ($13.31 \pm 1.81 \mu\text{m}$, $n=18$), *: $P < 0.05$. Middle, Nav1.2 length in 20 mmol/L glucose-treated group ($23.97 \pm 1.61 \mu\text{m}$, $n=36$) was similar to that in control group ($22.61 \pm 1.98 \mu\text{m}$, $n=18$), ns: $P > 0.05$. Right, distal end of Nav1.2 in 20 mmol/L glucose-treated group ($42.85 \pm 2.08 \mu\text{m}$, $n=36$) was similar to that in control group ($35.92 \pm 2.21 \mu\text{m}$, $n=18$), *: $P < 0.05$.

- C. Schematic of AnkG and Nav1.2 position in dendritic AISs in rats. AnkG, pink filled box, Nav1.2, green filled box.
- D. In dendritic AIS neurons in mice, compared with control group (gray), AIS was slightly distally located in 3 h 20 mmol/L glucose-treated group (pink), while AIS length was similar. Left, proximal end of AIS in 20 mmol/L glucose-treated group ($33.22 \pm 2.77 \mu\text{m}$, $n=29$) was more distally located than that in control group ($25.72 \pm 1.41 \mu\text{m}$, $n=24$), *: $P < 0.05$. Middle, AIS length in 20 mmol/L glucose-treated group ($30.25 \pm 1.72 \mu\text{m}$, $n=29$) was similar to that in control group ($33.05 \pm 1.57 \mu\text{m}$, $n=24$), ns: $P > 0.05$. Right, distal end of AIS in 20 mmol/L glucose-treated group ($63.47 \pm 3.12 \mu\text{m}$, $n=29$) was similar to that in control group ($58.77 \pm 1.91 \mu\text{m}$, $n=24$), ns: $P > 0.05$.
- E. In dendritic AIS neurons in mice, compared with control group (gray), both Nav1.2 location and length were similar to 3 h 20 mmol/L glucose-treated group (pink). Left, proximal end of Nav1.2 in 20 mmol/L glucose-treated group ($25.03 \pm 1.61 \mu\text{m}$, $n=20$) was similar to that in control group ($28.17 \pm 1.60 \mu\text{m}$, $n=18$), ns: $P > 0.05$. Middle, Nav1.2 length in 20 mmol/L glucose-treated group ($33.11 \pm 2.42 \mu\text{m}$, $n=20$) was similar to that in control group ($27.96 \pm 1.79 \mu\text{m}$, $n=18$), ns: $P > 0.05$. Right, distal end of Nav1.2 in 20 mmol/L glucose-treated group ($58.14 \pm 3.12 \mu\text{m}$, $n=20$) was similar to that in control group ($56.13 \pm 2.38 \mu\text{m}$, $n=18$), ns: $P > 0.05$.
- F. Schematic of AnkG and Nav1.2 position in dendritic AISs in mice. AnkG, pink box, Nav1.2, green box.

Error bars represent SEM; two-tailed unpaired *t*-test was employed in A-B and D-E.

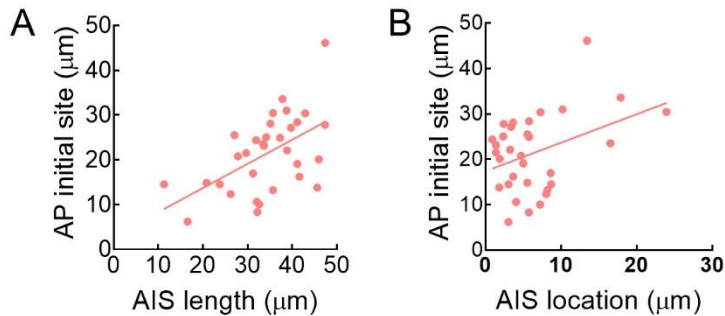


Supplementary Figure S4 Changes in velocity of AP propagation in dendrites were resolved well using voltage imaging

- A.** CheRiff-P2A-QuasAr2-mOrange2 (Optopatch2) (Hochbaum et al., 2014) was expressed in neurons to monitor AP propagation in dendrites. Panels from left to right show bright field image and fluorescence channels of mOrange2, CheRiff-EGPF, and QuasAr2, respectively. Scale bar: 20 μm .
- B.** Synchronized voltage imaging in simulated neuron with optogenetics. Left panel, ROIs selected in neurons are highlighted with different colors: blue: soma; orange, yellow, and purple: three ROIs in different dendrites adjacent to soma. Right panel, synchronized voltage imaging data from four ROIs corresponding to optogenetic stimulation (highlighted with light blue lines on top, 0.05 W/cm²). Data were acquired at 464 Hz.
- C.** AP propagation was resolved well after upsampling. Left panel, 1 000 times upsampling average optical signal (interval=2 μs) in four ROIs was calculated by averaging multiple AP spikes shown in (b) with the same processing pathway described in Fig. 1. Here,

fluorescence intensity of the four ROIs was normalized. Right panel, AP propagation map showing clear propagation pattern from soma to dendrites.

- D.** Snapshots of average AP movies after upsampling processing; interval of four images is 0.1 ms (red represents arrival of AP on pixels).
- E.** AP propagation in a single dendrite. Left panel, selected dendrites in fluorescence image (QuasAr2 channel) are highlighted in white, and centerline of dendrite is labeled with red asterisks; middle panel, distance-to-soma AP spike timing plot at selected dendrites. Note, AP spike timings at different spatial acquisition units (red asterisks) reside in a time duration of less than one raw frame (2.1535 ms), and average “pitch” between different spatial acquisition units in these dendrites is approximately 3.7 μm . Right panel, x-t curve of selected dendrites. Red dots are the same as red asterisks in the other two columns, and solid blue line represents x-t relationship after smoothing. Clear non-uniform (deceleration) propagation from soma to distal dendrite is observed on the curve, highlighted by blue and red dashed circles.



Supplementary Figure S5 APs were initiated more distally in longer/distally located AISs.

- A.** Correlation of AIS length and AP initiation site ($n=32$, $r=0.5372$, **: $P<0.01$).
- B.** Correlation of AIS location and AP initiation site ($n=32$, $r=0.3820$, *: $P<0.05$).

Supplementary Table S1. Spectral properties and filter sets of stains and fluorescent proteins used in this study.

Fluorophore	Excitation max. (nm)	Emission max. (nm)	Laser excitation wavelength (nm)	Emission filter (nm)
DAPI	350	470	405	460/50
Alexa Fluor® 405	401	421	405	460/50
Alexa Fluor® 488	490	525	488	525/50
mOrange2 (Shaner et al., 2008)	549	565	532	585/65
Alexa Fluor® 568	578	603	561	600/37
QuasAr2 (Hochbaum et al., 2014)	590	715	637	700/75
Alexa Fluor® 647	650	665	637	700/75

Dichroic mirror: Chroma ZT405/488/561/640rpc and ZT405/488/532/642rpc

Supplementary Table S2. Model parameters in Figure 4D-J

Compartment	Diameter × length ($\mu\text{m} \times \mu\text{m} \mu\text{m} \times \mu\text{m}$)	G_{Na} ($\text{pS}/\mu\text{m}^2$ pS/ μm^2)	G_{K} ($\text{pS}/\mu\text{m}^2$ pS/ μm^2)
dendrite	2×1000	100	20
soma	20×40	100	20
dendrite2	1.5 (0.8~2) ×1000	100	20
AIS	1.2 (0.8~2) ×40 (20~80)	5000	1000
axon	1.2 (0.6~2) ×1000	300	150

General parameters: C_m (specific membrane capacitance): 0.5 $\mu\text{F}/\text{cm}^2$; R_m (specific membrane resistance): 10000 $\Omega \cdot \text{cm}^2$; R_a (intracellular resistivity): 300 $\Omega \cdot \text{cm}$; E_L (leak reversal potential): -65 mV

Supplementary Table S3. Model parameters in Figure 5E and F

Compartment	diameter×length ($\mu\text{m} \times \mu\text{m} \mu\text{m} \times$ μm)	G_{Na} ($\text{pS}/\mu\text{m}^2$ pS/ μm^2)	G_{K} (pS/μ m^2 pS/ μm^2)
left cable	20×500	1200	360
(somatic)	2×50	1200	360
middle cable (dendritic)	3×50	1200	360
middle cable right cable	20×450	1200	360

General parameters: C_m (specific membrane capacitance): 1.0 $\mu\text{F}/\text{cm}^2$; R_m (specific membrane resistance): 1000 $\Omega \cdot \text{cm}^2$; R_a (intracellular resistivity): 100 $\Omega \cdot \text{cm}$; E_L (leak reversal potential): -65 mV